Program Digest, 2019 IEEE International Ultrasonics Symposium (IUS)
Glasgow, Scotland, October 6-9, 2019

A New 3D Imaging Technique Integrating Ultrafast Compounding, Hadamard Encoding, and Reconfigurable Fresnel Lensing, demonstrated on a 128-Element, Crossed Electrode Endoscope

Katherine Latham
Biomedical Engineering
Dalhousie University
Halifax, NS, Canada
kate.latham@dal.ca

Christopher Samson
Biomedical Engineering
Dalhousie University
Halifax, NS, Canada
samsonchris.cs@gmail.com

Jeffrey Woodacre
Biomedical Engineering
Dalhousie University
Halifax, NS, Canada
jwoodacre@dal.ca

Eric Simpson
Biomedical Engineering
Dalhousie University
Halifax, NS, Canada
eric.simpson@dal.ca

Roger Zemp
Electrical and Computer Engineering
University of Alberta
Edmonton, AB, Canada
rzemp@ualberta.ca

Jeremy A. Brown
Biomedical Engineering, Electrical and Computer Engineering
Dalhousie University
Halifax, NS, Canada
j.brown@dal.ca

***Abstract*— Crossed electrode arrays address some the challenges associated with 3D ultrasound imaging because of the significant reduction in the number of elements ($2N\ vs.\ N^2$). However, creating a two-way focused 3D image in real-time is difficult with these arrays because azimuth and elevation dimensions cannot be beamformed at the same time. We have developed a new 3D imaging approach that uses the flexibility of bias sensitive substrates to create a high-quality elevation focus on a crossed electrode array. The principle behind this technique is to perform conventional compound imaging with an azimuth set of electrodes, while implementing a bias controllable elevation lens with an elevation set of electrodes. On transmit, the biases are chosen to mimic a Fresnel lens. Then, on receive, Hadamard coding is implemented along the elevation dimension. After decoding, we gain the RF data for each element across the elevation aperture even though there is effectively only one channel in that dimension. A 30MHz, 64x64 element crossed electrode relaxor array was fabricated on a semi-kerfed, electrostrictive substrate and was used to demonstrate the performance of the imaging technique. The -6dB beamwidths were simulated to be 155µm and 170µm in the azimuth and elevation direction respectively and the secondary lobe levels were suppressed below -50dB. Images were generated of a wire phantom to confirm the performance of the elevational focus with good agreement between simulation and experiment.**

Keywords—3D imaging, crossed electrode array, endoscope, electrostrictive, Hadamard coding

I. Introduction

3D ultrasound imaging presents various challenges surrounding fabricating and packaging an array with a large number of elements, electrically matching to the very small, high impedance elements and acquiring the volumetric image in real time. Most of these challenges become more difficult to overcome at higher operating frequencies and for endoscopic applications. Crossed electrode arrays require significantly fewer elements and electrical connections than a conventional 2D array ($2N\ vs.\ N^2$), for that reason, the array design addresses some of the challenges of 3D ultrasound imaging. However, creating a two-way focused 3D image in real-time is difficult with these arrays because azimuthal and elevational elements overlap and cannot be beamformed at the same time. This typically forces one to use a synthetic aperture approach which forces trade-offs between SNR, frame rate and a high quality, two-way elevation focus.

This work describes a new 3D imaging technique that performs ultrafast imaging with the elements along the azimuth while combining a bias controllable transmit lens and receive Hadamard coding using the elevational elements. The imaging technique is demonstrated on a 128-element crossed electrode array in a miniature, endoscopic form factor.

II. Imaging Methods

We have developed a new 3D imaging approach that uses the flexibility of bias sensitive (i.e. pulse amplitude and polarity depend on a DC bias) substrates to create a high-quality elevation focus on a crossed electrode array. The principle behind this technique is to perform conventional compound imaging with an azimuth set of electrodes, while implementing a bias controllable elevation lens with an elevation set of electrodes. Fig. 1 shows the crossed electrode array architecture with the signal and bias channels assigned to the top and bottom electrodes respectively. On transmit, the biases are chosen to mimic a Fresnel lens. Then, on receive, Hadamard coding is implemented along the elevation dimension. After N pulses

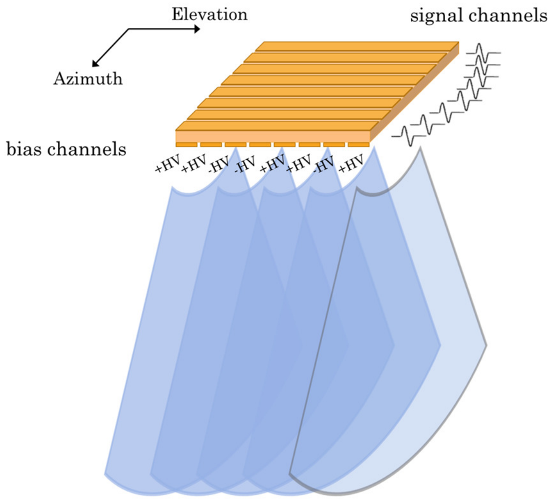

Fig. 1. Diagram showing the signal channels along the azimuth direction, bias channels along the elevation direction and slice-by-slice acquisition of a volume image.

and N orthogonal receive patterns the data can be decoded for the current image slice.

Hadamard based coding has been used in various forms in ultrasound imaging, first largely to improve SNR in synthetic aperture imaging [1] and, more recently, to provide a transmit elevation focus on crossed electrode arrays [2], [3]. A Hadamard matrix is made up of entries equal to +1 or -1 with the property that each row is mutually orthogonal. When the elements across an aperture, in this case the receive elevation, are Hadamard encoded (given either a positive or negative polarity) we can perform a simple matrix calculation on the set of received signals to decode and retrieve the equivalent of the RF data from each element across the array. The decoding steps uses the properties of orthogonal matrices. The transpose of an orthogonal matrix multiplied by the matrix is equal to an identity matrix with a gain term (2.

$$\boldsymbol{H^T H = nI} \tag{1}$$

The Hadamard matrix is given by $\boldsymbol{H}$, the column vector of RF data at time, t, received for each coded receive bias pattern is given by $\boldsymbol{R}$ (The received field across the elevation dimension, $\boldsymbol{F}$, at time, t, that has been coded by H) and the decoded RF data at time t for each element is given by $\boldsymbol{E}$.

$$\boldsymbol{H^T R}(t) = \boldsymbol{H^T H F(t)} = \boldsymbol{E}(t)$$

$$\boldsymbol{R}(t) = \begin{bmatrix} RF_{rx1} \\ RF_{rx2} \\ \vdots \\ RF_{rxN} \end{bmatrix}_t \quad , \quad \boldsymbol{E}(t) = \begin{bmatrix} RF_{ele1} \\ RF_{ele2} \\ \vdots \\ RF_{eleN} \end{bmatrix}_t \tag{2}$$

The decoding step results in the received signals from each elevational element, as if only one elevational element was active at a time on receive. With this data we form a synthetic receive aperture and can dynamically receive beamform at all image depths, with the added advantage of having 100% of the aperture active during each transmit/receive event. On transmit, we create a focus with the Fresnel lens so, in sum, a two-way focus is created. This process is repeated for each elevational slice in the 3D image. Using 64 elevational elements (corresponding to 64 orthogonal receive codes) and 32 elevation slices, this technique has a potential frame rate of 19.5 volumes/s. Implementing a synthetic receive elevation aperture with a crossed electrode array requires the same number of transmit/receive events, however, only one elevational element is active for each receive. The number of transmits/receive events become costly when building a traditional two-way synthetic elevation aperture. The number of transmit event increase to N^2, rather than N. In an extended acquisition time, it can be difficult to maintain phase for compounding and the system becomes susceptible to motion artefacts. We can limit the acquisition to N pulses per elevational slice while maintaining an approximate two-way focus because we are using an electrically configurable, Fresnel mimicking lens on transmit.

The imaging technique was simulated using Field II. A 30MHz, 2D array was modelled to demonstrate the 3D imaging performance. The control over polarization was replicated by applying apodization values of either +1 or -1. The crossed electrode array architecture was modelled by applying the same delay profiles across elevational elements and the same apodization profiles across azimuthal elements. The receive

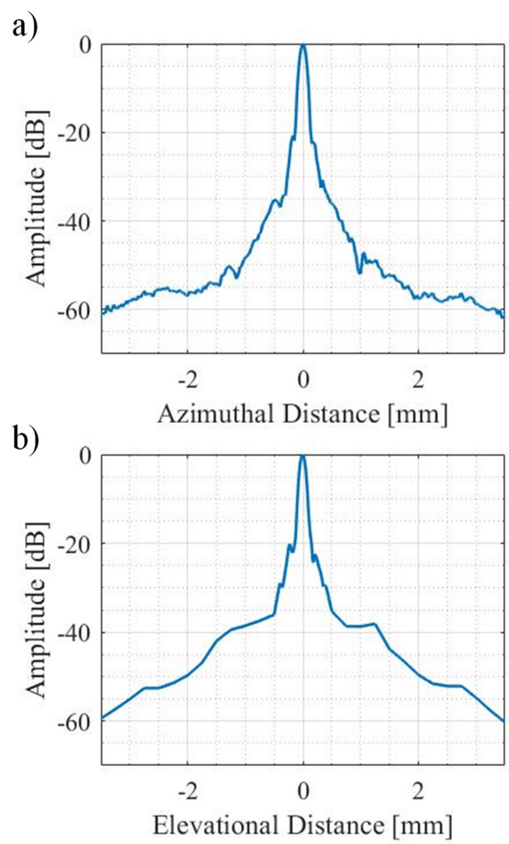

Fig. 2. Simulated radiation patterns a) along the azimuth direction and b) along the elevation direction.

signals across the elevational elements were summed to reduce the RF data to a signal channel in elevation for each azimuthal element. Simulated two-way radiation patterns in both imaging planes are shown in Fig. 2. The azimuthal and elevation -6dB beamwidths are 155 µm and 170 µm, respectively and the secondary lobe levels were suppressed below -50dB.

III. Imaging Array

A 30MHz, 64x64 element crossed electrode relaxor array was fabricated on a electrostrictive substrate. An electrostrictive array substrate was chosen because it has the unique property of being piezoelectric only when a DC bias is applied. Moreover, the pulse polarity is controlled with the sign of the DC bias. The elevation transmit lens and receive Hadamard coding is implemented using this property of the array material.

The array was designed with λ pitch and two matching layers. A process has been developed that uses a thinly diced strip of flex circuit to bring the back-side connections to the common bond surface, which allows the final size of the endoscope to measure only 5.0 x 5.0 mm. The array packaged into the endoscopic form factor is shown in Fig. 3. The inset in Fig. 3 highlights the miniature packaging made possible by the compact electrical connections. The electrical impedance of the electrostrictive array elements measured 30 ohms on resonance with a peak phase angle of -35 degrees. A two-way pulse bandwidth of 57% was measured using an echo returning from a wire target.

Previous studies have reported problems arising from being unable to produce pulses that are perfectly inverted [4] (i.e. maintains the same amplitude and shape). The electrostrictive ceramic material has the advantage that, since the polarization within the material changes direction with bias, it can produce perfectly inverted pulses. Therefore, it is an ideal candidate for this type of spatial coding, even on commercial systems where the transmit pulse shape cannot be altered channel to channel.

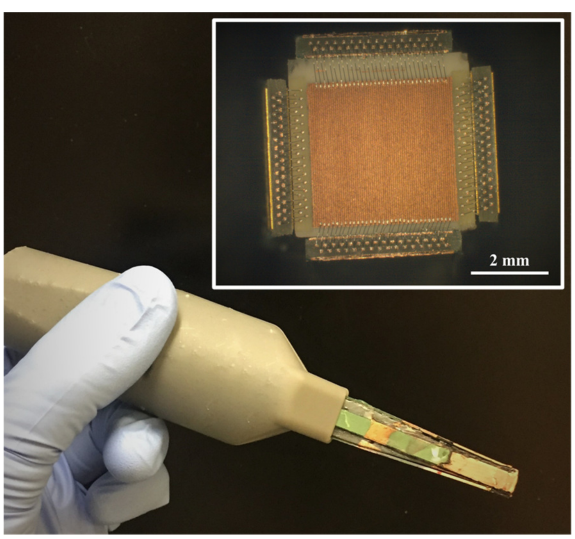

Fig. 3. Photo of the array packaged into the endoscopic for factor and (inset) the face of the array with the wire bonds completed.

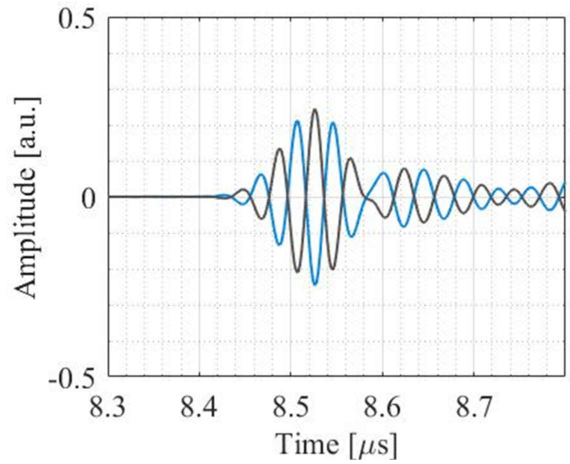

Fig. 4. Pulse echo data demonstrating the symmetry of the inverted pulse

Fig. 4 demonstrates the pulse inversion on an experimental pulse echo. Both pulses are transmitted with a positive bias voltage but one echo is received after switching to a negative bias between transmit and receive. In addition, the biases can be switched very quickly. The material generates over 90% of the full piezoelectric response less than 4 µs after applying or inverting the bias.

IV. Imaging Experiment

Imaging performance was tested using a custom 64 channel beamforming system with a 3D imaging module that provides the 64 reconfigurable, fast switching biasing channels. 3D images were generated by imaging a wire phantom using a reconfigurable acoustic Fresnel lens and Hadamard receive coding to focus to a series of elevation slices and build the volume image slice by slice. An ultrafast compounding scheme

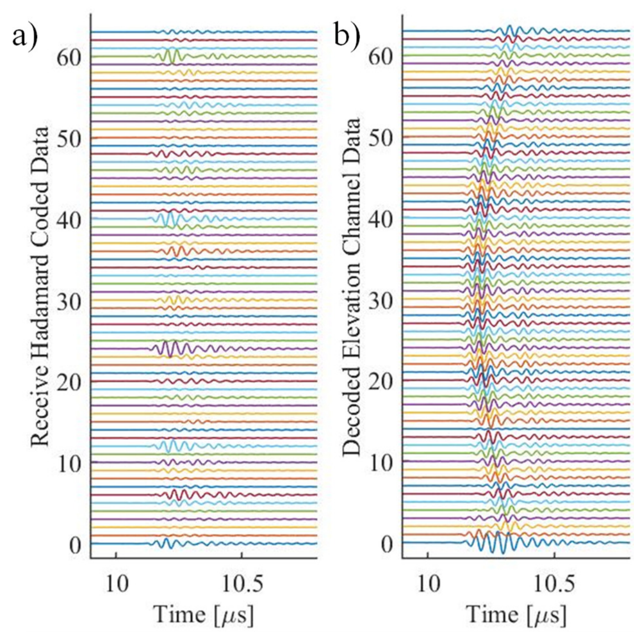

Fig. 5. Data after N insonifications collected from an example signal channel and displayed a) before decoding and b) after Hadamard decoding.

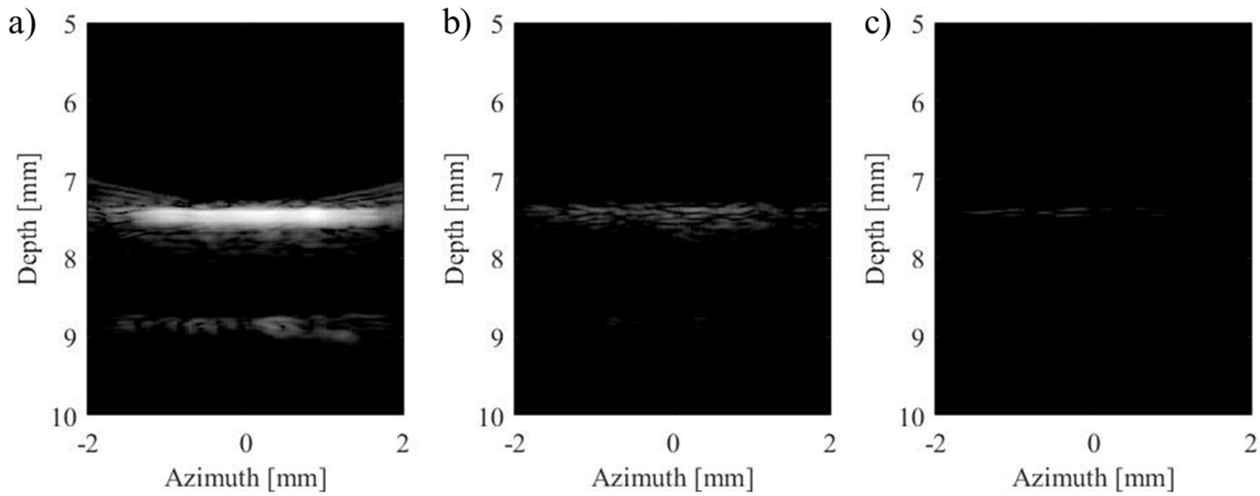

Fig. 6. Images of a wire phantom a) on the elevational axis, b) 0.5 mm off axis and, c) 1 mm off axis. The images are displayed with 45dB dynamic range.

was implemented in the azimuth direction using diverging waves. In both the elevation and azimuth directions, 64 insonifications were used to compound and reconstruct each 2D slice.

V. Results and Discussion

Data was collected from wire phantoms in a water bath. The N receive coded data sets from all N signal channels were stored then decoded and beamformed offline. Fig. 5 shows the data received by a representative element before and after decoding. After decoding the data becomes uniform in amplitude and has the appropriate delay profile for the reflection from a point target.

Radiation pattern data was collected to compare against the simulated data shown in Fig. 2 b) by imaging a wire stretched across the azimuthal elements. Frames of data focused to the elevational centre were collected on-axis, at 0.5 mm and 1 mm off-axis. The resulting images are shown in Fig. 6. The maximum beamformed signal is reduced to -27 dB at 0.5 mm and -42 dB at 1 mm. The corresponding simulation data (See Fig. 2) points are -36 dB and -39 dB at 0.5 mm and 1 mm respectively.

While these results show promise for this imaging technique, more thorough testing of the imaging technique in both the azimuthal and elevational planes is ongoing. The planned tests include full point spread functions in both dimensions and volumetric phantom images. In order to decode properly the bulk transmit delays in the azimuth plane must be accounted for. Experiments are ongoing to ensure the beamforming system, the electrostrictive crossed electrode array and the reconstruction algorithm are working together in this complex imaging technique.

VI. Conclusion

For crossed electrode arrays, accessing channel data in the elevation dimension is key for providing a high-quality elevation focus and an isotropic point spread function for the volume image. An electrostrictive substrate can be used to provide an electrically configurable elevation focus in a novel way. Combining a Fresnel lens on transmit with receive Hadamard coding allows a two-way focus to be created in the elevation dimension of these 2D arrays. In addition, the elevation plane can be dynamically receive beamformed without sacrificing SNR by performing conventional synthetic aperture.

References

[1] R. Y. Chiao, L. J. Thomas, and S. D. Silverstein, "Sparse array imaging with spatially-encoded transmits," in *1997 IEEE Ultrasonics Symposium*, 1997, pp. 1679–1682.

[2] C. Ceroici, T. Harrison, and R. J. Zemp, "Fast Orthogonal Row-Column Electronic Scanning With Top-Orthogonal-to-Bottom Electrode Arrays," *IEEE Trans. Ultrason. Ferroelectr. Freq. Control*, vol. 64, no. 6, pp. 1009–1014, 2017.

[3] C. Ceroici, K. Latham, B. Greenlay, J. A. Brown, and R. Zemp, "Fast Orthogonal Row-Column Electronic Scanning (FORCES) Experiments and Comparisons," *Submitt. Publ.*

[4] T. Harrison, A. Sampaleanu, and R. J. Zemp, "S-Sequence Spatially-Encoded Synthetic Aperture Ultrasound Imaging," *IEEE Trans. Ultrason. Ferroelectr. Freq. Control*, vol. 61, no. 5, pp. 886–890, 2014.